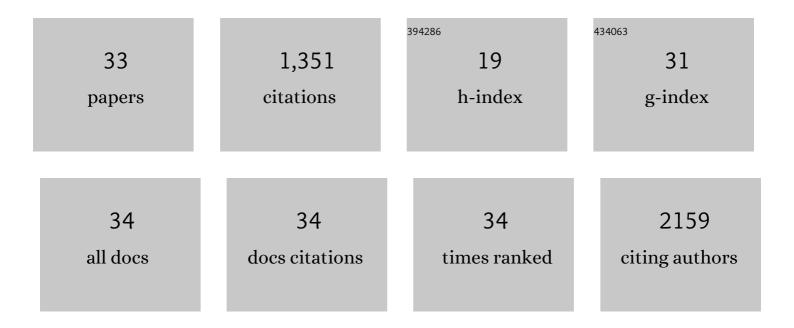
## **Michael Peller**

List of Publications by Year in descending order

Source: https://exaly.com/author-pdf/6861317/publications.pdf Version: 2024-02-01



#	Article	IF	CITATIONS
1	Imparting Functionality to MOF Nanoparticles by External Surface Selective Covalent Attachment of Polymers. Chemistry of Materials, 2016, 28, 3318-3326.	3.2	218
2	Thermosensitive liposomal drug delivery systems: state of the art review. International Journal of Nanomedicine, 2014, 9, 4387.	3.3	203
3	Size of thermosensitive liposomes influences content release. Journal of Controlled Release, 2010, 147, 436-443.	4.8	106
4	Metal–organic framework nanoparticles for magnetic resonance imaging. Inorganic Chemistry Frontiers, 2018, 5, 1760-1779.	3.0	99
5	Optimization and evaluation of the signal intensity change in multisection oxygen-enhanced MR lung imaging. Magnetic Resonance in Medicine, 2000, 43, 860-866.	1.9	96
6	Non-invasive temperature mapping using MRI: comparison of two methods based on chemical shift and T1-relaxation. Magnetic Resonance Imaging, 1998, 16, 393-403.	1.0	77
7	Oxygen-enhanced MRI of the brain. Magnetic Resonance in Medicine, 2002, 48, 271-277.	1.9	54
8	Method of hyperthermia and tumor size influence effectiveness of doxorubicin release from thermosensitive liposomes in experimental tumors. Journal of Controlled Release, 2016, 222, 47-55.	4.8	50
9	T1 relaxation time at 0.2 Tesla for monitoring regional hyperthermia: Feasibility study in muscle and adipose tissue. Magnetic Resonance in Medicine, 2002, 47, 1194-1201.	1.9	40
10	Surrogate MRI markers for hyperthermia-induced release of doxorubicin from thermosensitive liposomes in tumors. Journal of Controlled Release, 2016, 237, 138-146.	4.8	40
11	MR Characterization of Mild Hyperthermia-Induced Gadodiamide Release From Thermosensitive Liposomes in Solid Tumors. Investigative Radiology, 2008, 43, 877-892.	3.5	39
12	Hyperthermia induces T1 relaxation and blood flow changes in tumors. A MRI thermometry study in vivo. Magnetic Resonance Imaging, 2003, 21, 545-551.	1.0	37
13	Fast oxygen-enhanced multislice imaging of the lung using parallel acquisition techniques. Magnetic Resonance in Medicine, 2005, 53, 1317-1325.	1.9	35
14	Non-ionic Gd-based MRI contrast agents are optimal for encapsulation into phosphatidyldiglycerol-based thermosensitive liposomes. Journal of Controlled Release, 2013, 166, 22-29.	4.8	27
15	Quantitative, Multi-institutional Evaluation of MR Thermometry Accuracy for Deep-Pelvic MR-Hyperthermia Systems Operating in Multi-vendor MR-systems Using a New Anthropomorphic Phantom. Cancers, 2019, 11, 1709.	1.7	27
16	Regional Relative Blood Volume MR Maps of Meningiomas Before and After Partial Embolization. Journal of Computer Assisted Tomography, 1998, 22, 104-110.	0.5	24
17	<i>In vitro</i> characterization of phosphatidylglyceroglycerolâ€based thermosensitive liposomes with encapsulated <sup>1</sup> H MR <i>T</i> <sub>1</sub> â€shortening gadodiamide. Contrast Media and Molecular Imaging, 2008, 3, 19-26.	0.4	23
18	A pilot trial of doxorubicin containing phosphatidyldiglycerol based thermosensitive liposomes in spontaneous feline soft tissue sarcoma. International Journal of Hyperthermia, 2017, 33, 178-190.	1.1	22

MICHAEL PELLER

#	Article	IF	CITATIONS
19	Oxygen-induced MR signal changes in murine tumors. Magnetic Resonance Imaging, 1998, 16, 799-809.	1.0	20
20	Ferrite-enhanced MRI monitoring in hyperthermia. Magnetic Resonance Imaging, 2005, 23, 1017-1020.	1.0	19
21	Clinically Approved MRI Contrast Agents as Imaging Labels for a Porous Ironâ€Based MOF Nanocarrier: A Systematic Investigation in a Clinical MRI Setting. Advanced Therapeutics, 2020, 3, 1900126.	1.6	19
22	Tuning the Morphological Appearance of Iron(III) Fumarate: Impact on Material Characteristics and Biocompatibility. Chemistry of Materials, 2020, 32, 2253-2263.	3.2	19
23	Analysis of Signal Dynamics in Oxygen-Enhanced Magnetic Resonance Imaging. Investigative Radiology, 2010, 45, 165-173.	3.5	12
24	A Heatâ€Activated Drugâ€Delivery Platform Based on Phosphatidylâ€{oligo)â€glycerol Nanocarrier for Effective Cancer Treatment. Advanced NanoBiomed Research, 2021, 1, 2000089.	1.7	12
25	Effects of partial volume and phase shift between fat and water in gradient-echo magnetic resonance-mammography. Magnetic Resonance Materials in Physics, Biology, and Medicine, 1996, 4, 105-113.	1.1	8
26	MRIâ€Active Metalâ€Organic Frameworks: Concepts for the Translation from Lab to Clinic. Advanced Therapeutics, 2021, 4, 2100067.	1.6	6
27	Tuning the Synergistic Interplay between Clinical MRI Contrast Agents and MR-Active Metal–Organic Framework Nanoparticles. Chemistry of Materials, 2022, 34, 3862-3871.	3.2	6
28	Flip angle-optimized fast dynamic T <sub>1</sub> mapping with a 3D gradient echo sequence. Magnetic Resonance in Medicine, 2015, 73, 1158-1163.	1.9	5
29	A multi-institution study: comparison of the heating patterns of five different MR-guided deep hyperthermia systems using an anthropomorphic phantom. International Journal of Hyperthermia, 2020, 37, 1103-1115.	1.1	5
30	Material Characterization of Dual-Energy Computed Tomographic Data Using Polar Coordinates. Journal of Computer Assisted Tomography, 2015, 39, 134-139.	0.5	1
31	REDUCE – Indication catalogue based ordering of chest radiographs in intensive care units. Journal of Critical Care, 2022, 69, 154016.	1.0	1
32	New drugs for BNCT: An experimental approach. Strahlentherapie Und Onkologie, 1999, 175, 118-120.	1.0	0
33	Comparison Study of Oxygen-Induced MRI-Signal Changes and pO2 Changes in Murine Tumors. Advances in Experimental Medicine and Biology, 2003, 530, 461-465.	0.8	0